

Different Properties for Poly(3,4-ethylenedioxythiophene) Films Derived from Single or Multiple Polymerization Steps

David Aradilla,^{1,2} Francesc Estrany,^{2,3} Carlos Alemán^{1,2}

¹Departament d'Enginyeria Química, Escola Tècnica Superior (ETS) d'Enginyers Industrials, Universitat Politècnica de Catalunya, Diagonal 647, Barcelona 08028, Spain

²Center for Research in Nano-Engineering, Universitat Politècnica de Catalunya, Campus Sud, Edifici C', C/Pasqual i Vila s/n, Barcelona E-08028, Spain

³Unitat de Química Industrial, Escola Universitària d'Enginyeria Tècnica Industrial de Barcelona, Universitat Politècnica de Catalunya, Comte d'Urgell 187, Barcelona 08036, Spain

Received 3 September 2010; accepted 14 November 2010

DOI 10.1002/app.33758

Published online 14 March 2011 in Wiley Online Library (wileyonlinelibrary.com).

ABSTRACT: Films of poly(3,4-ethylenedioxythiophene) were prepared with single and multiple electropolymerization steps, where the numbers of polymerization steps (n 's) were 3, 5, and 7, with identical experimental conditions and total polymerization times (τ 's). The electroactivity of the films prepared with multiple steps remained almost unaltered when n increased, with the ability of the films to store charge with $n > 3$ being smaller than that of the films with similar thicknesses but derived from a single electrodeposition step. In contrast, the stability of the films produced with n polymerization steps was significantly higher than that of the films derived from a single step with the same τ , with the difference between the two

systems increasing with n , that is, τ used to yield the films. On the other hand, although the morphological and topological characteristics of the surface and the electrical conductivity were affected by the procedure used to produce the films, the organization of the polymer molecules in the crystalline phase, the thermal stability, and the electronic properties (ionization potential, electron affinity, and lowest π - π^* transition energy) were practically identical in both cases. © 2011 Wiley Periodicals, Inc. *J Appl Polym Sci* 121: 1982–1991, 2011

Key words: conducting polymers; electrochemistry; layer growth; morphology

INTRODUCTION

Among conducting polymers (CPs), poly(3,4-ethylenedioxythiophene) (PEDOT; Scheme 1) is one of the most important because of its many advantages, including its excellent electrochemical properties, good transparency, excellent stability, high electrical conductivity (κ), and easy processing.^{1–6} Consequently, this material, which can be prepared with chemical and electrochemical methods, has attracted considerable interest, and many applications based on these properties have been rapidly developed, for example, antistatic coatings, electrode materials in supercapacitors, hole-injection layers in organic light-emitting diodes, and solar cells.^{7–10}

On the other hand, the layer-by-layer technique based on electrostatic or other molecular forces creates an advantageous approach to constructing different types of self-assembled materials. Since the technique was first developed by Decher and coworkers,^{11–14} it has been successfully applied to fabricate ultrathin multilayered films of polyconjugated polymers.^{15–25} Within this context, films fabricated by the electrostatic self-assembly of PEDOT–poly(styrene sulfonate) and a polyelectrolyte, typically, poly(allylamine hydrochloride), are the most studied.^{21–25} Furthermore, conducting multilayered ultrathin films involving polypyrrole^{17,18} have been also reported.

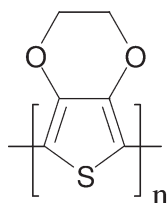
Recently, we used the electrochemical layer-by-layer technique to fabricate films formed by alternated layers of two different CPs through their electrodeposition.^{26,27} Thus, individual anodic polymerization processes, which were developed with two electrochemical cells containing solutions of different monomers, were used to prepare films formed by layers of different polymers. The thickness of each layer was controlled through the polymerization time used to generate it (τ_i), extending from a few nanometers to some micrometers. Specifically, we prepared multilayered systems made of PEDOT and

Correspondence to: F. Estrany (francesc.estrany@upc.edu) or C. Alemán (carlos.aleman@upc.edu).

Contract grant sponsor: (MICINN) Ministerio de Ciencia e Innovación and (FEDER) Fondo Europeo de Desarrollo regional funds; contract grant number: MAT2009-09138.

Contract grant sponsor: Generalitat de Catalunya (research group 2009 SGR 925 and XRQTC) Xarxa de Referència en Química Teòrica i Computacional).

Contract grant sponsor: (FPU-UPC) Formación Personal Investigador-Universitat Politècnica de Catalunya (for D.A.).



PEDOT

Scheme 1

poly(*N*-methylpyrrole) (PNMPy), abbreviated as ml-PEDOT/PNMPy, which showed an excellent ability to store charge (electroactivity) and a very high electrochemical stability (electroactivity). Indeed, the properties of ml-PEDOT/PNMPy were considerably better than those reported for the individual homopolymers and copolymers prepared with different mass ratios.^{5,28,29} The excellent properties of ml-PEDOT/PNMPy systems were attributed to the interface between the PEDOT and PNMPy layers. Thus, the coupling between the layers made of different CPs was, in terms of enhancement of the properties, significantly more positive than the interaction between the corresponding monomers in copolymers.

In this study, we extended our previous work on ml-PEDOT/PNMPy systems, examining and comparing the properties of films made of a single CP but prepared with one or multiple electrodeposition steps (n is the number of polymerization steps). Specifically, we focused on PEDOT, which is more electroactive and stable than PNMPy. Notably, PEDOT films produced with n polymerization steps can be viewed as n -layered systems made of a single CP. However, in this case, no evidence of the existence of multilayers can be provided, which is an important difference with respect to systems made of two different CPs. To facilitate the comparison with ml-PEDOT/PNMPy systems; hereafter, we refer to PEDOT films produced with a single and multiple polymerization steps as 1-films and n -films, respectively. The results obtained in this study, together with those reported for ml-PEDOT/PNMPy,^{26,27} gave us knowledge about the relative importance of two factors in the improvement of the properties: the influence of the second CP versus the effect of the multiple-step polymerization procedure.

EXPERIMENTAL

Materials

3,4-Ethylenedioxythiophene (EDOT) and acetonitrile (analytical-reagent grade) were purchased from Aldrich, St. Louis (USA) and were used without further purification. LiClO₄ (analytical-reagent grade, Aldrich) was stored in an oven at 80°C before use in the electrochemical trials.

Polymerization

The anodic polymerization of PEDOT was studied by cyclic voltammetry (CV) and chronoamperometry (CA) with a VersaStat II potentiostat–galvanostat (801 South Illinois Avenue, Oak Ridge, TN 37831-0895 USA) connected to a computer controlled through a Power Suite Princeton Applied Research program, (Princeton Applied Research, 801 South Illinois Avenue, Oak Ridge, TN 37830). Electrochemical experiments were conducted in a three-electrode, two-compartment cell under a nitrogen atmosphere (99.995% pure) at 25°C. The anodic compartment was filled with 40 mL of a 0.01M EDOT solution in acetonitrile containing 0.1M LiClO₄ as a supporting electrolyte, whereas the cathodic compartment was filled with 10 mL of the same electrolyte solution. Steel AISI 316 sheets of 4 cm² in area were used as working and counter electrodes. To prevent interferences during the electrochemical analyses, the working and counter electrodes were cleaned with acetone before each trial. The reference electrode was an Ag|AgCl electrode containing a KCl saturated aqueous solution (offset potential versus the standard hydrogen electrode, ($E^{\circ} = 0.222$ Volts (V) at 25°C) and was connected to the working compartment through a salt bridge containing the electrolyte solution.

PEDOT was generated by CA under a constant potential of 1.40 V, which was reported to be the optimum oxidation potential for the experimental conditions used in this study.²⁸ The thickness of the films (ℓ) was controlled through the total polymerization time (τ). PEDOT films prepared with a single polymerization step (1-films) were obtained with τ 's of 300, 500, and 700 s. The generation of the n -films was performed with n polymerization steps. In the first step, the working electrode was immersed for a period of time (τ_1) in a cell filled with an acetonitrile solution of EDOT with 0.1M LiClO₄, the same solution that was used for subsequent polymerization steps. τ of the film corresponded to the sum of the polymerization times for all of the steps: In this study, n -films were formed with three, five, and seven polymerization steps, with τ_1 being 100 s in all cases.

To investigate the effect of the monomer concentration in the solution on the properties of the n -films, some additional tests were performed with a fresh solution for every polymerization step. Interestingly, the electrochemical (electroactivity and electroactivity), morphological, and topographical properties of the n -films prepared with a single monomer solution and n fresh solutions were practically identical (data not shown). This was because τ_1 was very small, and therefore, the variation of the concentration of the monomer in the solution was negligible. This feature was demonstrated by chronoamperograms recorded for the oxidation of the

different systems prepared in this study, which were practically identical in all cases.

ℓ values and electrochemical and electrical properties

ℓ was estimated from the mass of the polymer deposited in the electrode (m_{pol}) with the procedure reported by Schirmeisen and Beck.³⁰ Accordingly, m_{pol} was determined with the following relation:

$$m_{\text{pol}} = Q_{\text{pol}} \left(\frac{m}{Q} \right) \quad (1)$$

where Q_{pol} is the polymerization charge consumed in the generation of each layer (mC/cm^2) and m/Q is the current productivity ($0.875 \text{ mg}/\text{C}$ for PEDOT prepared with identical experimental conditions).⁵ The volume of polymer deposited in the electrode (V_{pol}) was obtained with the values of m_{pol} and the density ($1.66 \text{ g}/\text{cm}^3$ for PEDOT).⁵

The electroactivity and electrostability were determined by CV with an acetonitrile solution with $0.1M$ LiClO_4 . The initial and final potentials were -0.50 V, whereas reversal potentials of 1.60 and 2.00 V were considered. The electroactivity increased with the similarity between the anodic and cathodic areas of the first control voltammogram, whereas the electrostability decreased with the oxidation and reduction areas of the consecutive control voltammograms. A scan rate of $100 \text{ mV}/\text{s}$ was used in all cases. κ was determined with the sheet-resistance method following a previously described procedure.³¹

Morphological and structural characterization

Morphological studies were performed with scanning electron microscopy (SEM) and atomic force microscopy (AFM) operating in tapping mode. Topographic AFM images were obtained with a Molecular Imaging PicoSPM with a NanoScope IV controller (Veeco, 100 Sunnyside Blvd. Ste. B Woodbury, New York, 11797-2902, USA) under ambient conditions. The average RMS (root mean square) roughness (r) was determined with the statistical application of the Nanoscope software, which calculated the average by considering all the values recorded in the topographic image with exception of the maximum and the minimum. Thus, with a surface in the horizontal plane assumed, root mean square (RMS) roughness was defined as the root mean squared value of all vertical deviations from the mean surface level. Measurements were conducted under ambient conditions at about 50% relative humidity and at 20 – 22°C . The system was placed on an active vibration isolation table for minimum acoustic disturbance (20 series, TMC, Peabody, MA). SEM images were achieved with a Focused Ion

Beam Zeiss Neon40 scanning electron microscope (Oberkochen, Germany) operating at a 5-kV accelerating voltage.

X-ray diffraction (XRD) spectra were recorded with a Bruker D8 Advance model (5465 East Cheryl Parkway Madison, WI 53711-5373, USA) at 40 kV and 40 mA ($\lambda = 1.5406 \text{ \AA}$). The XRD patterns were recorded under ambient conditions with 10 s per angular step ($1 \text{ angular step} = 0.02^\circ$).

Thermal analysis

The thermal stability was examined by thermogravimetric analysis (TGA) with a PerkinElmer TGA-6 thermobalance (Massachusetts, USA) at a heating rate of $20^\circ\text{C}/\text{min}$ under a nitrogen atmosphere.

Quantum mechanical calculations

Complete geometry optimizations of neutral $(\text{EDOT})_n$ oligomers, where n refers to the number of repeating units, were performed with the antiplanar conformation as a starting geometry; that is, all of the interring dihedral angles ($\text{S}-\text{C}-\text{C}-\text{S}$) were initially set at 180° .^{32,33} Calculations were performed with the B3LYP functional^{34,35} combined with the 6-31G(d) basis set.³⁶

The lowest $\pi-\pi^*$ electron transition energies (ε_g 's) were obtained with two different strategies. In the first one, ε_g was estimated with Koopmans' theorem (KT)³⁷ as the difference between the energy of the highest occupied molecular orbital ($\varepsilon_{\text{HOMO}}$) and the energy of the lowest unoccupied molecular orbital ($\varepsilon_{\text{LUMO}}$), that is, $\varepsilon_g = \varepsilon_{\text{HOMO}} - \varepsilon_{\text{LUMO}}$, obtained at the B3LYP/6-31G(d) level of theory. Thus, Levy and Nagy³⁸ evidenced that ε_g could be rightly estimated by this procedure with density functional theory calculations. In the second strategy, ε_g was evaluated with the time-dependent density functional theory (TD-DFT) to evaluate the electronic excitations. Both KT and TD-DFT estimations were obtained at the Boese–Martin for kinetics (BMK) level of theory, which is based on the generalized gradient functional BMK,³⁹ combined with the 6-31G(d) basis set with the geometries optimized at the B3LYP/6-31G(d) level.

RESULTS AND DISCUSSION

Electrochemical characterization of the PEDOT systems

n -Films of PEDOT produced with the experimental procedure previously described were rinsed several times with acetonitrile, dried under a nitrogen flow, and immersed in the electrolyte solution of the control cell for CV analysis. The chronoamperogram obtained for the oxidation of 1- and 3-films with a constant applied potential of 1.4 V and a τ of 300 s

TABLE I
 κ , ℓ , and r Values of 1- and n -Films Prepared in This Study

Material	κ (S/cm) ^a	ℓ (μm) ^a	r (nm) ^a
3-Film ($\tau = 300$ s)	129	2.79	529
1-Film ($\tau = 300$ s)	107	2.21	368
1-Film ($\tau = 400$ s)	102	2.84	332
5-Film ($\tau = 500$ s)	128	3.92	352
1-Film ($\tau = 500$ s)	110	3.40	310
7-Film ($\tau = 700$ s)	125	6.03	266
1-Film ($\tau = 700$ s)	103	5.45	218

In all cases, the films were produced on a steel substrate by CA with a constant potential of 1.40 V and a total polymerization time τ .

^a We obtained the σ_0 , ℓ , and r values listed in Table I by averaging five samples.

indicated that the anodic current density, which stabilized at 1.46 mA/cm² (data not shown) in the two systems, was not affected by n . Despite this, the average ℓ of the n -films was larger than that of the 1-films prepared with identical experimental conditions. This is reflected in Table I, which shows that ℓ values determined for the n -films with $n = 3, 5,$ and 7 were 26, 15, and 11% larger, respectively, than those of the 1-films prepared with $\tau = 300, 500,$ and 700 s, respectively. Thus, the impact of the growing effects associated with each polymerization step decreased when n increased.

Figure 1 compares the typical control voltammograms of the 1- and n -films prepared as described previously with $\tau = 300$ and 700 s. Determination of the cathodic and anodic areas indicated that the electroactivity of the 3-film was 9% higher than that of the 1-film produced with $\tau = 300$ s [Fig. 1(a)]. However, the opposite behavior was detected when the n - and 1-films obtained with higher polymerization times were compared [Fig. 1(b)]. More specifically, the electroactivities of the 1-films produced with $\tau = 500$ and 700 s were 7 and 9% higher, respectively, than those of the 5- and 7-films. This change in the electrochemical behavior was attributed to the negative influence of the interfaces in the electroactivity of the n -films. Thus, the electroactivity only grew 2 and 4% when n increased from $n = 3$ to $n = 5$ and 7 , respectively. Accordingly, the enhancement of the electroactivity with n was negligible, although ℓ grew with n . To eliminate the effect of the thickness from the discussion of the multistep effect, in Figure 1(c), we compare the 1-film prepared with $\tau = 400$ s with the 3-film obtained with $\tau = 300$ s. The electroactivity of the former was 4% higher than that of the latter, although the ℓ values determined for these two systems differed by only 0.05 μm (Table I). The behavior observed for the n -films of PEDOT was completely different from that reported for ml-PEDOT/PNMPy, in which the elec-

troactivity increased significantly and rapidly with the number of layers.²⁷ Thus, comparison between the n -films of PEDOT and ml-PEDOT/PNMPy films allowed us to conclude that the ability to store charge was only enhanced by interfaces involving two different CPs.

1-Films prepared with $\tau = 400, 500,$ and 700 s were more electroactive than those yielded with $\tau = 300$ s by 7, 16, and 20%, respectively. This feature was consistent with previous observations, which indicated that the electroactivity of 1-films grew very rapidly with τ until a threshold thickness of $\ell \approx 4$ μm was reached and explained the variation in the electrochemical behavior displayed in Figure 1 for the n - and 1-films.

We investigated the electrochemical stability of the n -films by applying 30 consecutive oxidation–reduction

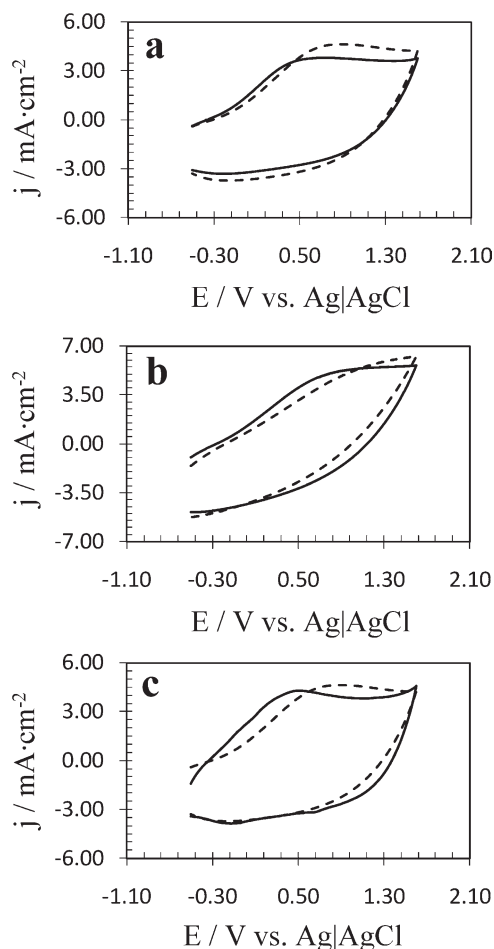


Figure 1 Control voltammograms for the oxidation of the n - and 1-films: (a) 3- (dashed line) and 1-films (solid line) prepared with $\tau = 300$ s, (b) 7- (dashed line) and 1-films (solid line) generated with $\tau = 700$ s, and (c) 3- (dashed line) and 1-films (solid line) generated with $\tau = 300$ s and 400 s, respectively. Voltammograms were recorded with a 4-cm² steel electrode in acetonitrile with 0.1M LiClO₄ at 100 mV/s and 25°C. Initial and final potentials = -0.50 V; reversal potential = 1.60 V (volts).

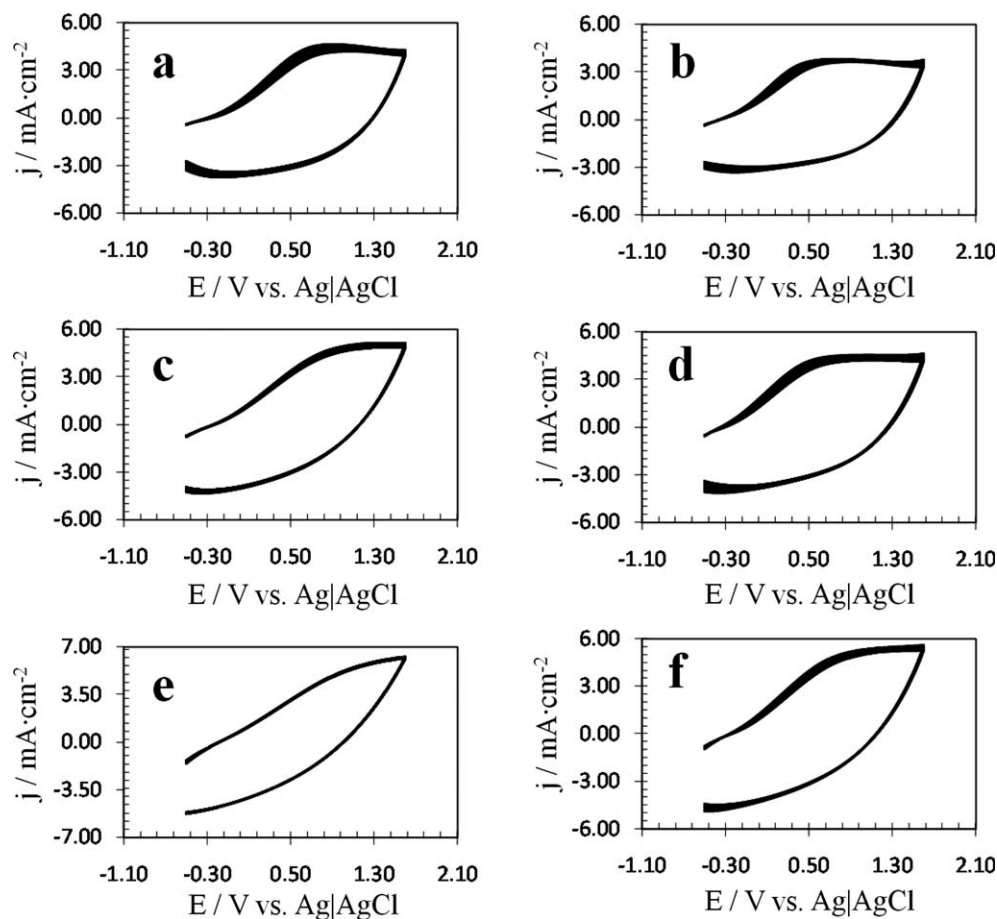


Figure 2 Control voltammograms for 30 consecutive oxidation–reduction cycles of the *n*- (left) and 1-films (right): (a) 3-film, (b) 1-film with $\tau = 300$ s, (c) 5-film, (d) 1-film with $\tau = 500$ s, (e) 7-film, and (f) 1-film with $\tau = 700$ s. The voltammograms were recorded with a 4-cm² steel electrode in acetonitrile with 0.1M LiClO₄ at 100 mV/s and 25°C. Initial and final potentials = -0.50 V; reversal potential = 1.60 V (volts).

cycles in the potential range from -0.50 to 1.60 V. In Figure 2, we compare the electrostability of the *n*-films ($n = 3, 5,$ and 7) and the 1-films yielded with $\tau = 300, 500,$ and 700 s. As shown, in all three cases, the electrostability of the *n*-film was higher than that of the corresponding 1-film, with the difference between the two systems increasing significantly with n and τ . Thus, for the 7-film, the loss of electroactivity upon 30 consecutive oxidation–reduction cycles was only 2%, whereas it was 11% for the 1-film prepared with $\tau = 700$ s. Table II provides a quantitative evaluation of these differences, which are expressed in terms of a loss of electroactivity. Similarly, the ml-PEDOT/PNMPy systems showed that the electrostability increased with the number of layers. On the other hand, the loss of electroactivity upon 30 consecutive oxidation–reduction cycles of the 1-film prepared with $\tau = 400$ s, which presented the same ℓ as the 3-film (Table I), was 15%. This value was practically identical to that obtained for the 3-film (Table II); this showed that the electrostability did not improve in the potential range under study.

Systematic electrochemical experiments showed that the difference between the electrostabilities of

the *n*- and 1-films became more important when the oxidation potential increased. This is reflected in Table III, which compares the electrostabilities obtained upon 30 consecutive oxidation–reduction cycles in the potential range from -0.50 to 2.00 V. Previous studies indicated that PEDOT films generated under the experimental conditions used in this study overoxidize when the oxidation potential is higher than 1.80 V.⁵ Despite this, the behavior described in Table III indicates, again, that the electrostability increases with n and τ , although in this case, the

TABLE II
Loss of Electroactivity after 30 Consecutive Oxidation–Reduction Cycles for the *n*- and 1-Films

<i>n</i> and τ (s)	<i>n</i> -Film (%)	1-Film (%)
$n = 3$ and $\tau = 300$ s	14	16
$n = 5$ and $\tau = 500$ s	8	14
$n = 7$ and $\tau = 700$ s	2	11

The potential range of the control voltammograms was -0.50 to 1.60 V.

TABLE III
Loss of Electroactivity after 30 Consecutive Oxidation-Reduction Cycles for the *n*- and 1-Films

<i>n</i> and τ (s)	<i>n</i> -Film (%)	1-Film (%)
<i>n</i> = 3 and τ = 300 s	36	51
<i>n</i> = 5 and τ = 500 s	22	48
<i>n</i> = 7 and τ = 700 s	12	41

The potential range of the control voltammograms was -0.50 to 2.00 V.

improvement was very remarkable for the *n*-films: the loss of electroactivity decreased from 36 to 12% when *n* increased from 3 to 7. For sake of comparison, the loss of electroactivity evolved from 51 to 41% when the τ used to prepare the 1-films increased from 300 to 700 s. Interestingly, a comparison of the 1- and 3-films with similar ℓ values ($\tau = 400$ and 300 s, respectively) indicated that the loss of electroactivity in the potential range from -0.50 to 2.00 V was 13% larger for the former than for the latter.

Morphology

Figures 3 and 4 compare the SEM micrographs of the 1- and *n*-films, respectively, prepared with $\tau = 300, 500,$ and 700 s, with the images being reproducible in all cases by the sampling of different regions

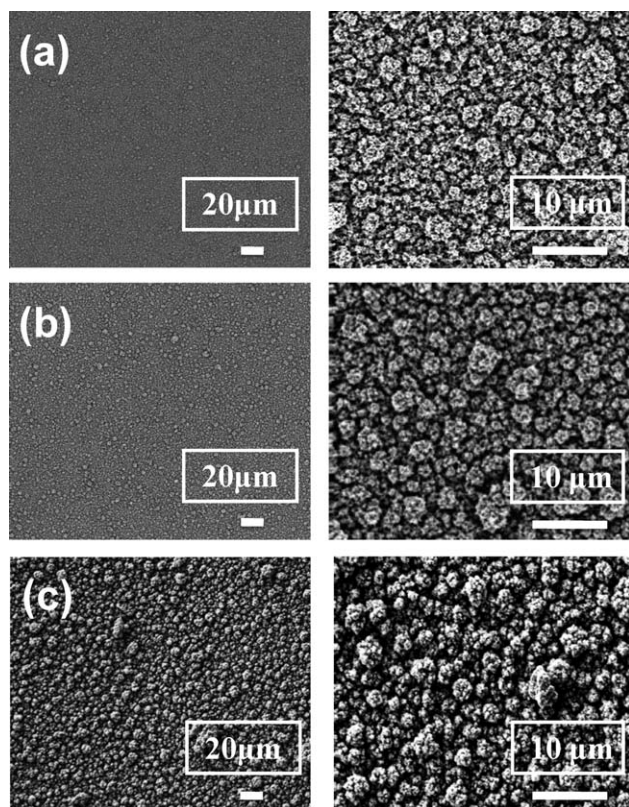


Figure 3 SEM micrographs of the 1-films prepared with $\tau =$ (a) 300, (b) 500, and (c) 700 s.

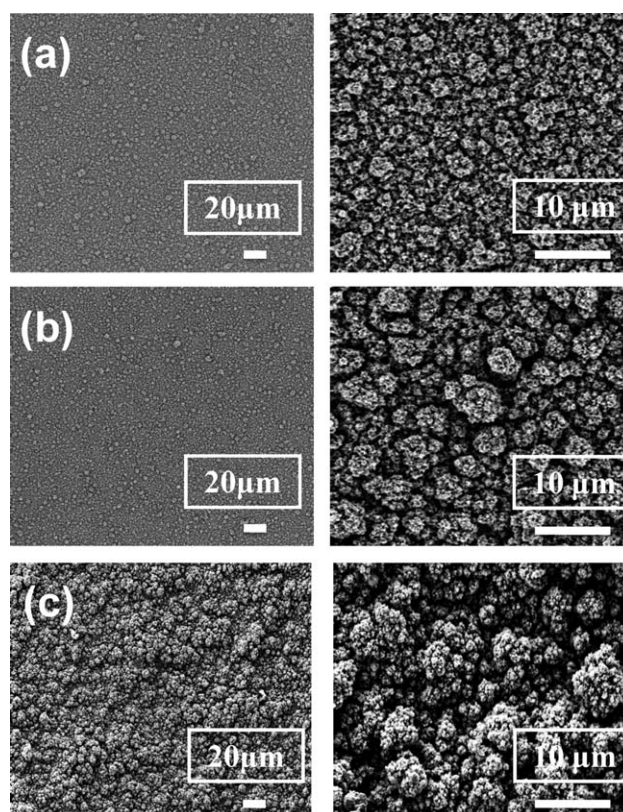


Figure 4 SEM micrographs of the *n*-films prepared with $\tau =$ (a) 300, (b) 500, and (c) 700 s.

of the films. The 1-films (Fig. 3) presented a compact granular surface, with the linear growing of the polymer chains being responsible for this uniform morphology. Thus, the PEDOT molecules were exclusively formed by α,α linkages because the dioxane ring fused onto the thiophene ring occupied the β positions of the latter. In the 1-films, rigid polymer molecules were grown through a continuous anodic polymerization process and favored the formation of dense and compact aggregates. Interestingly, large protuberances and high irregularities were observed in the surfaces of the *n*-films (Fig. 4). Thus, for each τ value, the density of the granules and agglomerates in the surface of the *n*-film was higher than that in the 1-film, although the difference between the two systems increased with *n*, as expected. Similarly, for a given τ , the diameter of the granules was larger in the *n*-film than in the 1-film, with the largest difference being found for $\tau = 700$ s; that is, in this case, the diameters for the 1- and 7-films were around 4 and 8 μm , respectively.

Figure 5 shows the tapping-mode AFM images of the 3-, 5-, and 7-films, whereas Table I compares *r* values determined for the 1- and *n*-films. As shown, in both cases, the roughness of the film decreased when ℓ increased. Thus, the roughness of the 7-film was about 50% smaller than that of the 3-film,

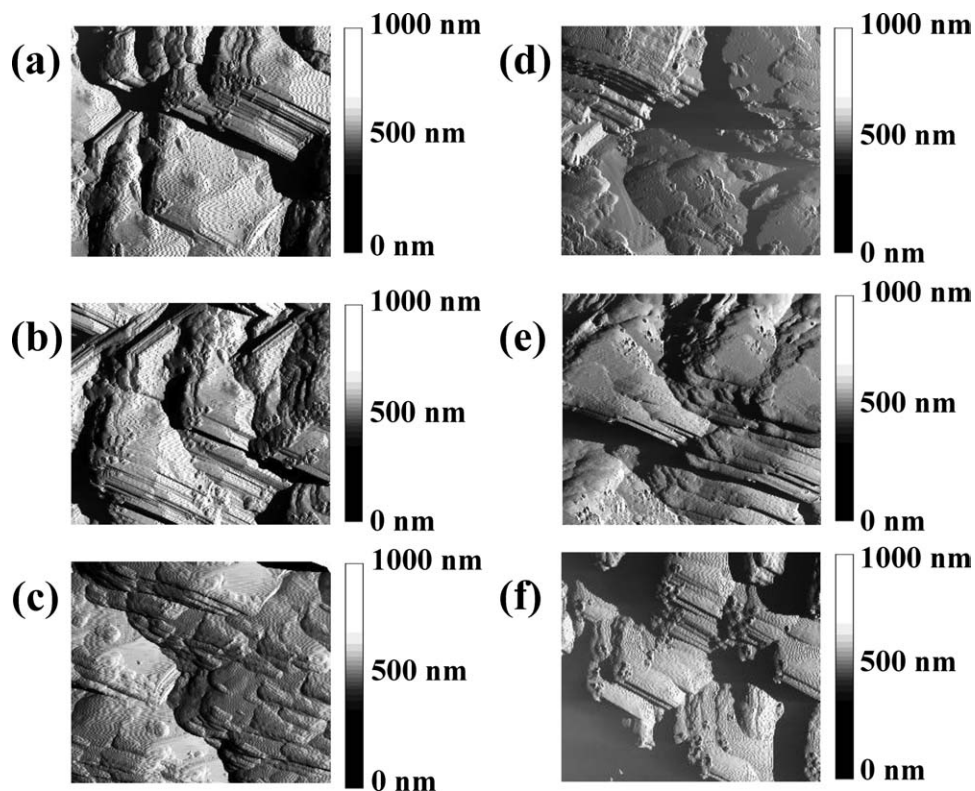


Figure 5 AFM images of the (a) 3-, (b) 5-, and (c) 7-films obtained with multiple polymerization steps and 1-films prepared with $\tau =$ (d) 300, (e) 500, and (f) 700 s. Scan size = 5 μm .

whereas the roughness of the 1-film prepared with $\tau = 300$ s was about 40% larger than that of the film produced with $\tau = 700$ s. These features are clearly reflected in Figure 5, which shows that the accentuated protuberances and irregular topography of the 3-film and the thinnest 1-film decreased when n and τ increased. On the other hand, the roughness of the 3-film was 161 \AA larger than that of the 1-film obtained with $\tau = 300$ s, although this difference decreased to less than 50 \AA when the n - and 1-films prepared with higher values of τ were compared. Thus, the difference in the roughness between the n - and 1-films decreased with the difference in ℓ of such films. The overall AFM results were consistent with the SEM micrographs discussed previously.

Figure 6 compares the XRD patterns of the 3- and 1-films produced with $\tau = 300$ s. The two spectra were very similar, showing a sharp peak centered at $2\theta = 6.3^\circ$, which corresponded to the (100) reflection, and two broad peaks at $2\theta = 12.6$ and 26.2° , which corresponded to the (200) and (002) reflections, respectively. These experimental peaks were fully consistent with the orthorhombic unit cell ($a = 14.0$ \AA , $b = 6.8$ \AA , and $c = 7.8$ \AA) reported for electrochemically generated PEDOT.^{40–42} Accordingly, the organization of the molecules in the crystalline phases was not altered by the differences in the polymerization process.

Thermal properties

The TGA curves of the 3- and 1-films generated with $\tau = 300$ s, which are displayed in Figure 7, were very similar and showed three different decomposition steps. The weight loss ($\sim 10\%$) associated with the first step corresponded to the evaporation of the acetonitrile solvent molecules trapped in the polymeric matrix, with this process occurring around 85°C . After this, a degradation process, which corresponded to the decomposition of linear

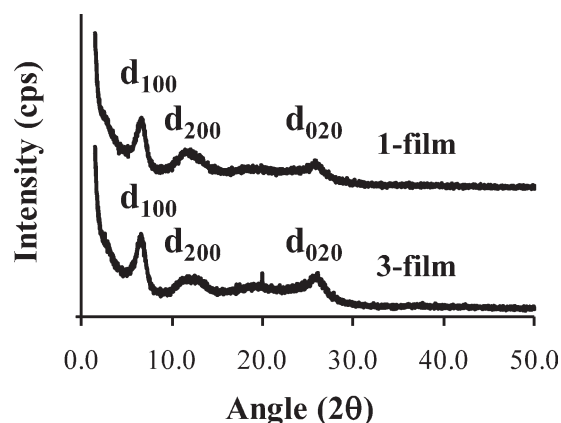


Figure 6 XRD patterns of the 3- and 1-films yielded with $\tau = 300$ s. d_{100} , d_{200} and d_{020} refer to interplanar spacings of the (100), (200) and (020) planes, respectively.

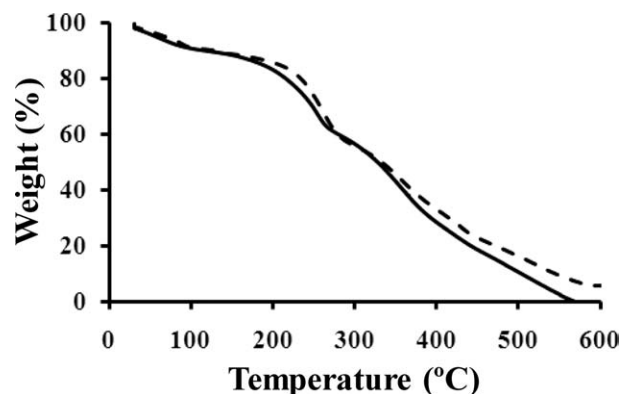


Figure 7 TGA of 3-(dashed line) and 1-films (solid line) prepared with $\tau = 300$ s.

segments of the polymer chains, began at about 200°C. Finally, the last degradation step started at about 350°C and should have been due to the decomposition of the ClO_4^- counterions; that is, the decomposition of LiClO_4 started at about 400°C. Thus, the remanent weight at 350°C, about 46%, should have been considered as the weight of ClO_4^- in the samples. This value was very close to the weight of ClO_4^- counterions previously determined by elemental analysis for 1-films of PEDOT prepared under identical experimental conditions.⁵

κ

The κ values determined for the PEDOT films prepared with a single or multiple polymerization steps are listed in Table I. The κ values determined for the n -films were around 127 S/cm in all cases, whereas the 1-films exhibited values around 107 S/cm. These results suggest that the electrodeposition in multiple steps produced a slight enhancement in κ . Figure 8 compares the temporal stability of the κ values of the 3-film and the corresponding 1-film. As shown, the relative reduction of κ was similar for the two

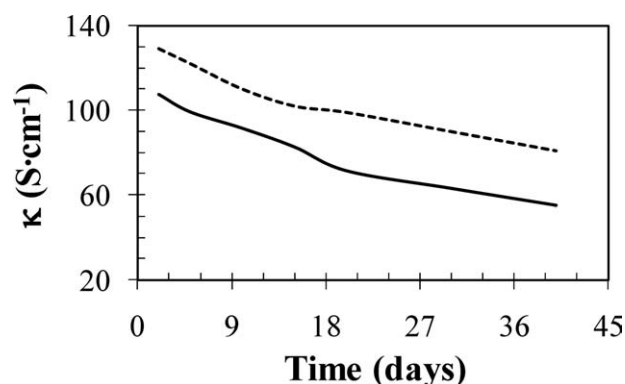


Figure 8 Temporal evolution of κ (S/cm) for the 3-film (dashed line) and 1-films (solid line) prepared with $\tau = 300$ s.

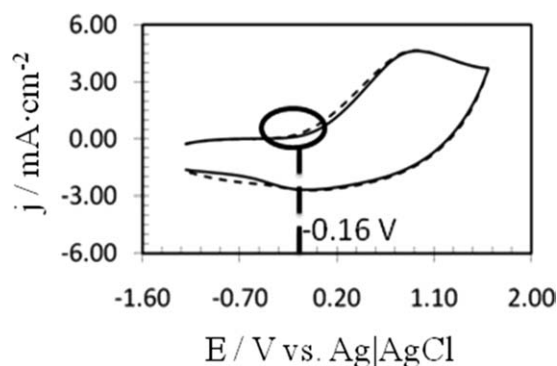


Figure 9 Control voltammograms for the oxidation of 3-film (dashed line) and 1-films (solid line) prepared with $\tau = 300$ s. Voltammograms were recorded with a 4-cm² steel electrode in acetonitrile with 0.1M LiClO_4 at 100 mV/s and 25°C. Initial and final potentials = -1.20 V; reversal potential = 1.60 V (volts).

systems; that is, after 40 days, the κ values were 81 and 55 S/cm, respectively.

Electronic properties

Electrochemical measures can be used to derive important electronic properties of CPs, for example, ionization potential (IP), electronic affinity (EA), or ϵ_g .^{43–46} According to Brédas et al.,⁴⁷ the IP and EA (both in eV) can be estimated with the following equations: $\text{IP} = E_{\text{ox}} + 4.4$ and $\text{EA} = E_{\text{red}} + 4.4$, which eliminate the environmental effects from oxidation (E_{ox}) and reduction (E_{red}) onsets (vs Ag|AgCl). The value of E_{ox} was -0.16 V for both the 3- and 1-films obtained with $\tau = 300$ s (Fig. 9). Moreover, the n -films with higher values of n and 1-films generated with $\tau = 500$ and 700 s showed almost identical values (data not shown). Accordingly, the IP value estimated for the n - and 1-films prepared in this study was 4.28 eV. This value was in good agreement with a previous experimental observation (4.1 eV).⁴⁸ Figure 10(a) represents the variation of the IP, which was estimated with KT, against $1/n$ calculated for $(\text{EDOT})_n$ oligomers at the BMK/6-31G(d) level. Linear regression analysis [$\text{IP} = a(1/n) + b$, where a is the slope and b is the intercept at the y axis] allowed us to extrapolate the IP to an idealized PEDOT chain made of infinite repeating units. The resulting value, 4.01 eV, was in good agreement with the experimentally determined one; that is, the theoretical value was underestimated by 6% only. Moreover, the value predicted in this study with the BMK functional was significantly closer to the experimental estimation than that recently calculated with the B3LYP one (3.45 eV).³³

As the stability of the oxidation–reduction is essential to the application of the equations developed by Brédas et al., a value of $E_{\text{red}} = -2.1$ V was taken from

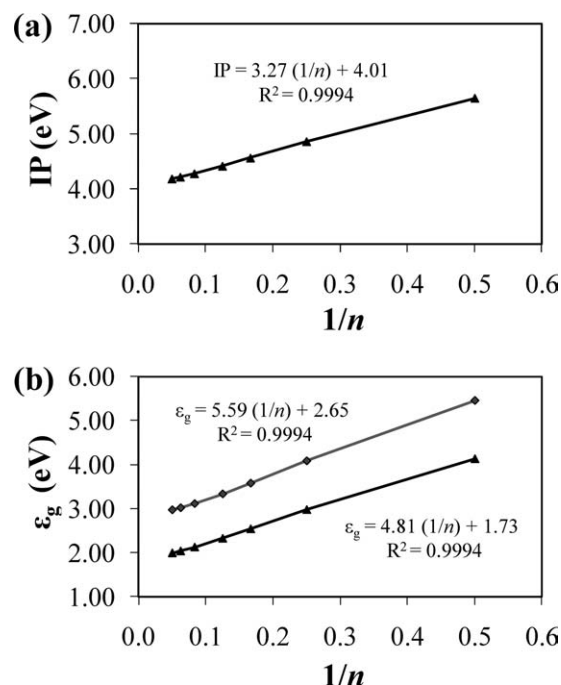


Figure 10 (a) IP (eV) calculated with KT at the BMK/6-31G(d) level plotted against the inverse number of repeating units ($1/n$) for $(\text{EDOT})_n$ (\blacktriangle). The line corresponds to the linear fit $\text{IP} = a(1/n) + b$. (b) Evolution of ϵ_g (eV) obtained with TD-BMK/6-31G(d) (\blacktriangle) and BMK/6-31G(d) calculations (\blacklozenge) plotted against the inverse number of repeating units ($1/n$) for $(\text{EDOT})_n$. The lines correspond to the linear fits $\epsilon_g = a(1/n) + b$.

the literature.⁴⁹ Accordingly, the estimated EA was 2.3 eV. ϵ_g , which was estimated as the difference between the IP and the EA, was 1.98 eV. The ϵ_g values determined for PEDOT with spectroscopic methods rather than electrochemical measures ranged from 1.60 to 1.70 eV.⁹ This feature suggests that the electronic properties derived from the electrochemical data were slightly overestimated with respect to the spectroscopic measures; this was a consequence of the drastic approximations introduced to evaluate the IP and EA.⁴⁷ Figure 10(b) represents the variation of the ϵ_g values calculated at the BMK/6-31G(d) level for the $(\text{EDOT})_n$ oligomers with the KT and TD-DFT strategies against $1/n$. Linear extrapolations allowed us to predict ϵ_g values of 2.65 (KT) and 1.73 eV (TD-DFT) for an infinite PEDOT chain. Thus, the ϵ_g derived from TD-DFT calculations was within the interval of reported experimental data, whereas the application of KT produced an overestimation of this electronic property. However, the results provided by KT depended dramatically on the functional, with the ϵ_g value recently derived at the B3LYP/6-31G(d) level being 1.66 eV.³³

CONCLUSIONS

The properties of PEDOT films prepared with multiple electropolymerization steps were compared

with those of films yielded through a continuous electropolymerization process. The results indicate that the electrochemical properties were drastically influenced by the polymerization method. The ability of the 1-films to store charge obtained with $\tau = 500$ and 700 s was higher than that of the 5- and 7-films, respectively. Moreover, the electroactivity of the n -films remained almost unaltered with increasing polymerization steps. This represented a significant difference with respect to the ml-PEDOT/PNMPy films, which showed not only that the electroactivity increased with the number of layers but also that multilayered films were considerably more electroactive than the corresponding monolayered ones.^{26,27} Accordingly, the presence of interfaces involving two different CPs enhanced the ability of the films to store charge, which was not achieved when the system was constituted by a single CP. On the other hand, the electrostability of the n -films was significantly higher than that of the 1-films, with the difference between the two systems increasing with n and τ . This observation was fully consistent with that reported for ml-PEDOT/PNMPy films.²⁷

The morphological characteristics and the roughness of the surface were influenced by the procedure used to grow the films. Thus, although both the n - and 1-films showed a granular morphology, protuberances and irregularities, that is, roughness, were more accentuated in the former than in the latter. Despite this, XRD indicated that the three-dimensional organization of the molecular chains in the crystalline phase was similar in both cases. On the other hand, κ was slightly larger in the n -films than in the 1-films. In contrast, the films prepared with a single and multiple polymerization steps presented similar thermal stability values and electronic properties.

The overall results presented in this article suggest that, in general, multilayered films prepared with two different CPs, for example, ml-PEDOT/PNMPy, present more advantages than n -films yielded with only one CP. However, for applications in which the electrostability and/or κ play an essential role, n -films are expected to be more successful than those obtained with the typical continuous electropolymerization process.

One of the authors (C.A.) acknowledges the Generalitat de Catalunya for their support of his research with the prize ICREA (Institutió Catalana de Recerca i Estudis Avançats) Academia for excellence in research.

References

- Jonas, F.; Shrader, L. *Synth Met* 1991, 41, 831.
- Heywang, G.; Jonas, F. *Adv Mater* 1992, 4, 116.
- Dietrich, M.; Heinze, J.; Heywang, G.; Jonas, F. *J Electroanal Chem* 1994, 369, 87.

4. Chiu, W. W.; Sejdic, J. T.; Cooney, R. P.; Bowmaker, G. A. *Synth Met* 2005, 155, 80.
5. Ocampo, C.; Oliver, R.; Armelin, E.; Alemán, C.; Estrany, F. *J Polym Res* 2006, 13, 193.
6. Tamburri, E.; Orlanducci, S.; Toschi, F.; Terranova, M. L.; Passeri, D. *Synth Met* 2009, 159, 406.
7. Brabec, C. J.; Sariciftci, N. S.; Hummelen, J. C. *Adv Funct Mater* 2001, 11, 15.
8. Granström, M.; Berggren, M.; Inganäs, O. *Science* 1995, 267, 1479.
9. Groenendaal, L.; Jonas, F.; Freitag, V.; Pielartzik, H.; Reynolds, J. R. *Adv Mater* 2000, 12, 481.
10. Groenendaal, L.; Zotti, G.; Aubert, P. H.; Waybright, S. M.; Reynolds, J. R. *Adv Mater* 2003, 15, 855.
11. Decher, G. *Science* 1997, 277, 1232.
12. Decher, G.; Hong, J. *Makromol Chem Macromol Symp* 1991, 46, 321.
13. Decher, G.; Hong, J. D.; Schmitt, J. *Thin Solid Films* 1992, 210, 831.
14. Decher, G.; Schmitt, J. *Prog Colloid Polym Sci* 1992, 89, 160.
15. Cheung, J. H.; Stockton, W. B.; Rubner, M. F. *Macromolecules* 1997, 30, 2712.
16. Fou, A. C.; Rubner, M. F. *Macromolecules* 1998, 28, 7115.
17. Zheng, S.; Tao, C.; He, Q.; Zhu, H.; Li, J. *Chem Mater* 2004, 16, 3766.
18. Zotti, G.; Vercelli, B.; Berlin, A. *Acc Chem Res* 2008, 41, 1098.
19. Zotti, G.; Zecchin, S.; Berlin, A.; Schiavon, G.; Giro, G. *Chem Mater* 2001, 13, 43.
20. Zotti, G.; Zecchin, S.; Schiavon, G.; Vercelli, B.; Berlin, A.; Porcio, W. *Chem Mater* 2004, 16, 2091.
21. Smith, R. R.; Smith, A.; Stricker, J. T.; Taylor, B. E.; Durstock, M. F. *Macromolecules* 2006, 39, 6071.
22. Stricker, J. T.; Gudmundsdóttir, A. D.; Smith, A. P.; Taylor, B. E.; Durstock, M. F. *J Phys Chem B* 2007, 111, 10397.
23. Wakizada, D.; Fushimi, T.; Ohkita, H.; Ito, S. *Polymer* 2004, 45, 8561.
24. DeLongchamp, D. M.; Kastantin, M.; Hammond, P. T. *Chem Mater* 2003, 15, 1575.
25. Jiang, G.; Baba, A.; Advincula, R. *Langmuir* 2007, 23, 817.
26. Estrany, F.; Aradilla, D.; Oliver, R.; Armelin, E.; Alemán, C. *Eur Polym J* 2008, 44, 1323.
27. Estrany, F.; Aradilla, D.; Oliver, R.; Alemán, C. *Eur Polym J* 2007, 43, 1876.
28. Oliver, R.; Muñoz, A.; Ocampo, C.; Alemán, C.; Estrany, F. *Chem Phys* 2006, 328, 299.
29. Ocampo, C.; Alemán, C.; Oliver, R.; Arnedillo, M. L.; Ruíz, O.; Estrany, F. *Polym Int* 2007, 56, 803.
30. Schirmeisen, M.; Beck, F. J. *J Appl Electrochem* 1989, 19, 401.
31. Carrasco, J.; Brillas, E.; Fernández, V.; Cabot, P. L.; Garrido, J. A.; Centellas, F.; Rodríguez, R. M. *J Electrochem Soc* 2001, 148, E19.
32. Casanovas, J.; Alemán, C. *J Phys Chem C* 2007, 111, 4823.
33. Carrión, S.; Rodríguez-Ropero, F.; Aradilla, D.; Zanuy, D.; Alemán, C. *J Phys Chem B* 2011, 114, 3494.
34. Becke, A. D. *J Chem Phys* 1993, 98, 1372.
35. Lee, C.; Yang, W.; Parr, R. G. *Phys Rev B* 1988, 37, 785.
36. Hariharan, P. C.; Pople, J. A. *Theor Chim Acta* 1973, 28, 213.
37. Koopmans, T. *Physica* 1934, 1, 104.
38. Levy, M.; Nagy, A. *Phys Rev A* 1999, 59, 1687.
39. Boese, A. D.; Martin, J. M. L. *J Chem Phys* 2004, 121, 3405.
40. Aasmundtveit, K. E.; Samuelsen, E. J.; Pettersson, L. A. A.; Inganäs, O.; Johansson, T.; Feidenhans, R. *Synth Met* 1999, 101, 561.
41. Feng, W.; Li, Y.; Wu, J.; Noda, H.; Fujii, A.; Ozaki, M.; Yoshino, K. *J Phys: Condens Matter* 2007, 19, 186220.
42. Niu, L.; Kvarnström, C.; Fröberg, K.; Ivaska, A. *Synth Met* 2001, 122, 425.
43. Micaroni, L.; Nart, F. C.; Hümmelgen, I. A. *J Solid State Electrochem* 2002, 7, 55.
44. Mello, R. M. Q.; Serbena, J. P. M.; Benvenho, A. R. V.; Hümmelgen, I. A. *J Solid State Electrochem* 2003, 7, 463.
45. Gruber, J.; Li, R. W. C.; Aguilar, L. H. J. M. C.; Garcia, T. L.; de Oliveira, H. P. M.; Atvars, T. D. Z.; Nogueira, A. F. *Synth Met* 2006, 156, 104.
46. Janietz, S.; Bradley, D. D. C.; Grell, M.; Giebeler, C.; Inbasekaran, M.; Woo, E. P. *Appl Phys Lett* 1998, 73, 17.
47. Brédas, J. L.; Silbey, R.; Boudreaux, D. S.; Chance, R. R. *J Am Chem Soc* 1983, 105, 6555.
48. Grenier, C. R. G.; Pisula, W.; Joncheray, T. J.; Müllen, K.; Reynolds, J. R. *Angew Chem Int Ed* 2007, 46, 714.
49. Ahonen, H. J.; Lukkari, J.; Kankare, J. *Macromolecules* 2000, 33, 6787.